CHEMISTRY
A EUROPEAN JOURNAL

DOI: 10.1002/chem.200900331

Conformational Flexibility of Tetralactam Macrocycles and Their Intermolecular Hydrogen-Bonding Patterns in the Solid State

Sascha S. Zhu,[a, b] Martin Nieger,[c] Jörg Daniels,[d] Thorsten Felder,[a] Iordan Kossev,[e] Thomas Schmidt,[f] Moritz Sokolowski,[e] Fritz Vögtle,[f] and Christoph A. Schalley*[a]

Abstract: Despite their rigid scaffold, tetralactam macrocycles (TLMs) display a remarkable degree of conformational flexibility, as revealed by analysis of the corresponding X-ray crystal structures. This flexibility is not limited to the rotatability of the TLM amide groups but also applies to the *m*-xylene rings, and it thus has a great impact on the overall shape of the macrocycle cavity. The conformational properties of the TLMs give rise to a broad variety of intermolecular hydrogen-bonding patterns, including infinite ladders, an interesting catemer motif, and short C–H···O=C hydrogen bonds. These results are in accord with previous theoretical calculations, support a structural model proposed earlier for an interpretation of scanning tunneling microscopy images, and substantially contribute to the understanding of the adaptability of macrocyclic scaffolds, which is crucial for guest binding or templated syntheses with TLMs.

Keywords: conformational flexibility · hydrogen bonds · macrocycles · supramolecular chemistry · tetralactams

Introduction

Since their first preparation more than a decade ago, Hunter's tetralactam macrocycles ("TLMs")[1,2] have gained more and more importance in supramolecular chemistry, because they are widely used not only as hosts for small guest molecules[1,3] but also as ring components in mechanically interlocked architectures, such as pseudorotaxanes,[4] rotaxanes,[5] and catenanes.[2,6] These easily accessible, chemically stable macrocycles bear four amide groups that are capable of forming hydrogen-bonding patterns, on which guest binding and templated syntheses of catenanes and rotaxanes are based.

According to theoretical calculations,[7] TLMs exhibit a certain degree of conformational flexibility, in that the amide groups and the *m*-xylene rings can quite easily be rotated. This essential structural feature certainly contributes to enhancing the versatility of TLMs as building blocks in supramolecular chemistry, because they keep their overall shape but can nevertheless adapt to the special steric requirements of their binding partners. One can safely assume that the secondary amide groups in the TLMs are *trans* configured. Rotation about the amide C–N bond is thus unfavorable. Theory predicts a barrier lower than 30 kJ mol^{-1} for rotation of the *whole* amide group from an A_{in} (with an amide group with the NH moiety converging into the cavity) into an A_{out} (with an amide NH moiety pointing away from the cavity) conformation. Consequently, an all-*in*, a 3-*in*-1-*out*, and two different 2-*in*-2-*out*[8] conformations are predicted to be accessible within an energy range of approximately 8 kJ mol^{-1}.[7] Significant strain is, however, generated when both amides of the same isophthalamide adopt

[a] Dipl.-Chem. S. S. Zhu, Dr. T. Felder, Prof. Dr. C. A. Schalley
Institut für Chemie und Biochemie, Freie Universität Berlin
Takustrasse 3, 14195 Berlin (Germany)
Fax: (+49) 30-838-55817
E-mail: schalley@chemie.fu-berlin.de

[b] Dipl.-Chem. S. S. Zhu
Current address:
Kekulé-Institut für Organische Chemie und Biochemie
Universität Bonn
Gerhard-Domagk-Strasse 1, 53121 Bonn (Germany)

[c] Dr. M. Nieger
Laboratory of Inorganic Chemistry, Department of Chemistry
P.O.Box 55, 00014 University of Helsinki (Finland)

[d] Dr. J. Daniels
Institut für Anorganische Chemie, Universität Bonn
Gerhard-Domagk-Strasse 1, 53121 Bonn (Germany)

[e] Dr. I. Kossev, Prof. Dr. M. Sokolowski
Institut für Physikalische und Theoretische Chemie, Universität Bonn
Wegelerstrasse 12, 53115 Bonn (Germany)

[f] Dr. T. Schmidt, Prof. Dr. F. Vögtle
Kekulé-Institut für Organische Chemie und Biochemie
Universität Bonn
Gerhard-Domagk-Strasse 1, 53121 Bonn (Germany)

the A_{out} conformation and so, for example, a 1-*in*-3-*out* conformation is unfavorable in energy. Herein, three aspects of these structural features are discussed, based on the X-ray crystal structures of TLMs **1**–**5** (Scheme 1): 1) the conformational freedom of the amide groups, 2) the effects of the presence of guests on the cavity shape and the orientation of the *m*-xylene rings, and 3) intermolecular hydrogen-bond formation in the crystals.

Results and Discussion

X-ray-quality crystals[9] of TLMs $\mathbf{4}^+$ and **5** (Scheme 1) were obtained in different ways: $\mathbf{4}^+$ was crystallized by slow evaporation of $CDCl_3$, whereas needlelike crystals of **5** were obtained through gradient vacuum sublimation at 1×10^{-5} mbar and a sublimation temperature of 600–630 K.[10] For comparison, we include the previously published crystal structures

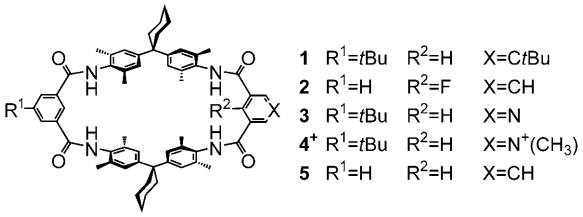

Scheme 1. Chemical structures of tetralactam macrocycles **1**–**5**.

of **1**,[11] **2**,[12] and **3**.[13] Note that TLM **3** is an exceptional case, because two different conformers (**3A** and **3B**) coexist in the crystal structure in a 1:2 ratio.

The first aspect to be discussed is the amide conformations in the solid state (Figure 1). The all-*in* conformer is observed for TLMs **1**, **3A**, and **5**, whereas **2** and **3B** adopt the 2-*in*-2-*out* conformation and $\mathbf{4}^+$ adopts the 3-*in*-1-*out* conformation. According to calculations,[7] the all-*in* conformation is the slightly more favorable one and enables the formation of two bifurcated hydrogen bonds for guest binding within the TLM cavity. Thus, this conformation was not only found in the crystal structures of **1** and **3A**, in which solvent molecules and Cl^- anions are hydrogen bonded to the four A_{in} protons. It is also observed in the crystal structures of TLM-containing [2]rotaxanes[14] and [2]pseudorotaxanes,[4] in which the axle is hydrogen bonded to the TLM part in the same manner. By contrast, the less common 3-*in*-1-*out* conformer has one "inverted" amide group, A_{out}, which can serve both as a hydrogen-bond donor for the exterior and as an acceptor for the interior of the cavity. The latter is essential for TLM-containing [2]catenanes, which form an interesting network of six hydrogen bonds between the two wheels. This pattern is not only observed in the crystal structures[6b,15] of the final catenanes but is also believed to play a pivotal role in their templated synthesis.[7] TLM $\mathbf{4}^+$ is unique in being the only TLM so far that displays a 3-*in*-1-*out* conformation in the solid state without being incorporated in a catenane. A second A_{out} group is present in the 2-*in*-2-*out* conformation, which has been observed in the solid-state

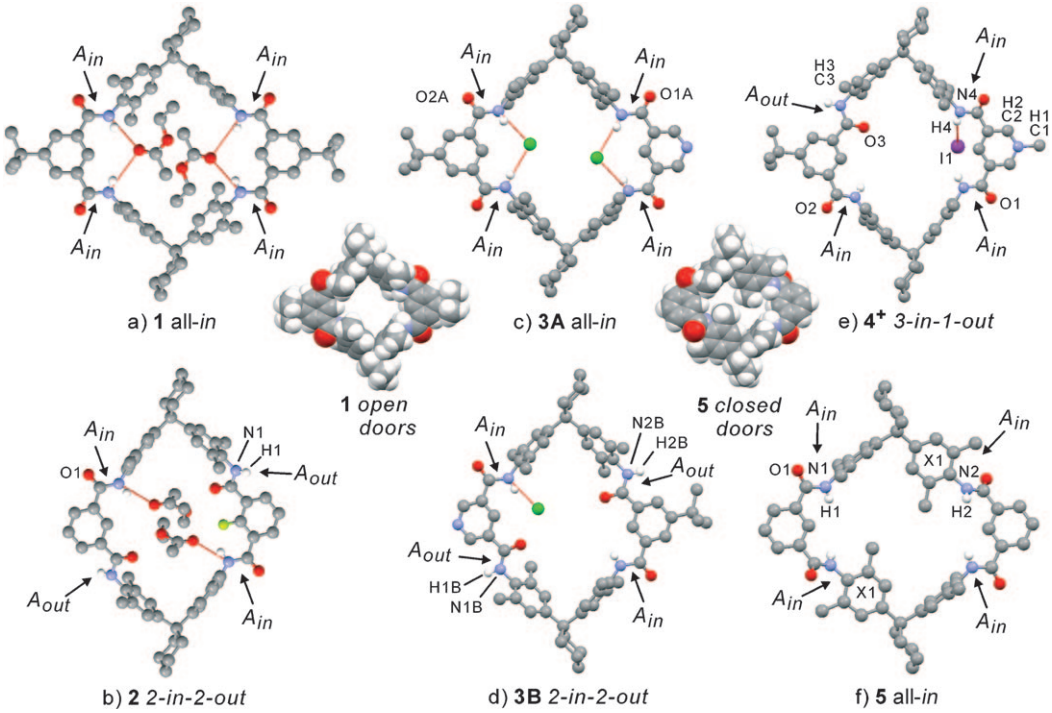

Figure 1. X-ray crystal structures of: a) **1**, b) **2**, c) **3A**, d) **3B**, e) $\mathbf{4}^+$, and f) **5**, all shown as ball-and-stick representations. Hydrogen bonds to guest molecules or anions are shown as red, dotted lines. Color code: C gray, Cl green, F yellow, H white, I purple, N blue, O red. H atoms (except amide protons) and other solvents or anions that are not hydrogen bonded to the TLMs are omitted for clarity. The two insets display the space-filling representations for **1** and **5**, to highlight the "open-doors" and "closed-doors" conformations.

structures of **2**[12] and **3** (conformer **3B**). This conformation is less effective for guest binding but facilitates the formation of intermolecular hydrogen-bond networks (for intermolecular hydrogen-bonding distances, see Table 1). Thus, the solid-state structures of **1**–**5** ideally confirm the theoretical predictions. The all-*in*, 3-*in*-1-*out*, and 2-*in*-2-*out* conformations all exist in the crystals and, therefore, must be quite close in energy and connected through rather low barriers for amide-group rotation.

Although the conformations of the amide groups affect the cavity shape by slightly distorting its rhomboid form, an overall open cavity is still retained, as long as the *m*-xylene moieties are more or less perpendicular to the overall plane of the macrocycle. In almost all crystal structures of TLMs known so far, guests such as solvent molecules or anions are present inside the cavity. The *m*-xylene rings accommodate the guests by adopting tilt angles of between 56° and 90° relative to the macrocycle plane[16] (Table 2). This is, for example, true for **1** and **2**, which both host two ethyl acetate molecules in their cavities (Figure 1a and b). Chloride anions are the guests in the crystal of **3**, which implies that at least some of the TLM pyridine rings are protonated. For **3A** and **3B**, the tilt angles are also within the range mentioned above. The only exception is the crystal of TLM **5**. This crystal was obtained by sublimation of the macrocycle and is thus—in contrast to all other examples—entirely free of solvent and guest molecules. In **5**, the two *m*-xylene rings (X1) are nearly coplanar with the macrocycle plane, with tilt angles as low as 4.6° (Figure 1f, Table 2). This causes the open macrocyclic cavity to be partly closed. We call this structure the "closed-doors" conformation. A comparison of the space-filling representations of the structures of **1** and **5** (insets in Figure 1) shows the differences between the open and the closed cavities. The closed-doors conformation of **5** might be advantageous in that it allows a more compact packing, but it is unsuitable for hosting guests. The marked differences in the tilt angles of the *m*-xylene rings depend on the presence of guest molecules and, thus, confirm that the macrocycle is quite easily able to adapt to the guest molecules' shapes.

The reason for the realization of different amide conformations is specific intermolecular hydrogen-bonding patterns (for H-bond lengths, see Table 1). The binding energy liberated upon the formation of intermolecular hydrogen bonds counterbalances the small energy differences between the different conformations. We will not discuss **1** here, because no intermolecular hydrogen bonds are found within the crystal. The all-*in* conformation in **1** merely results in the binding of two ethyl acetate molecules inside the cavity.

Besides the formation of one hydrogen bond to each of the two ethyl acetate guest molecules inside the cavity, the 2-*in*-2-*out* conformer in the crystal of **2** forms a pair of intermolecular N–H···O=C hydrogen bonds between the two symmetry-equivalent A_{out} H1 protons and A_{in} O1 oxygen atoms of two neighboring molecules. Each TLM molecule **2** is thus connected with its neighbors through a total of four hydrogen bonds and becomes a self-complementary building block, which assembles into a hydrogen-bonded homopolymer with the shape of an infinite ladder

Table 1. Intermolecular hydrogen bonds for **2**–**5**[a] between the atoms labeled in Figure 1. See also Figures 2–4.

	Donor–H···Acceptor (D–H···A)	*d*(D–H) [Å]	*d*(H···A) [Å]	*d*(D–A) [Å]	∢(DHA) [°]
2[b]	N1–H1···O1	0.89	2.13	3.01	171.5
3[b]	N1B–H1B···O1A[c]	0.88	1.99	2.85	166.7
	N2B–H2B···O2A[c]	0.88	1.98	2.81	157.0
4$^+$	N4–H4···I1$^-$	0.88	2.93	3.77	159.4
	C1–H1···O1	0.98	2.36	3.10	131.2
	C3–H3···O3	0.98	2.49	3.21	129.4
	C1–H1···O2	0.98	2.49	3.28	138.1
	C2–H2···O2	0.95	2.16	3.03	151.8
5[b]	N1–H1···O1	0.89	2.09	2.97	177.1
	N2–H2···O1	0.86	2.37	3.21	167.5

[a] Hydrogen bonds with a hydrogen···acceptor distance (*d*(H···A)) of more than 2.5 Å (except for amide–iodine interactions) are not listed in the table. [b] Symmetry transformations used to generate equivalent atoms: $-x+1$, $-y+1$, $-z+1$. [c] A and B denote the two crystallographically independent molecules found in the crystal of **3**.

Table 2. Tilt angles [°] relative to the macrocycle plane for **1**–**5**.

	Angles between the macrocycle plane and *m*-xylene planes[a]				Angles between the macrocycle plane and amide planes[b]			
1	60.4	60.4	83.1	83.1	16.7 (A_{in})	16.7 (A_{in})	30.7 (A_{in})	30.7 (A_{in})
2	68.8	68.8	75.0	75.0	32.6 (A_{in})	32.6 (A_{in})	44.4 (A_{out})	44.4 (A_{out})
3A[c]	82.9	82.9	85.9	85.9	11.5 (A_{in})	11.5 (A_{in})	24.7 (A_{in})	24.7 (A_{in})
3B[c]	56.2	64.4	70.6	86.2	11.0 (A_{out})	16.2 (A_{in})	16.5 (A_{out})	25.4 (A_{in})
4$^+$	77.9	80.8	82.5	87.9	8.1 (A_{out})	27.1 (A_{in})	27.4 (A_{in})	36.4 (A_{in})
5	4.6	4.6	88.7	88.7	22.8 (A_{in})	22.8 (A_{in})	50.3 (A_{in})	50.3 (A_{in})
Av.[d]			71.9				24.2 (A_{in}) 21.6 (A_{out})	

[a] The *m*-xylene plane is defined by the least-squares fit plane through all six aromatic carbon atoms of the corresponding *m*-xylene ring. [b] The amide plane is defined by the least-squares fit plane through the four atoms H–N–C=O of the corresponding amide group. [c] A and B denote the two crystallographically independent molecules found in the crystal of **3**. [d] Av.: Average value from the dataset of ten TLMs or TLM-containing compounds (X-ray structures of TLMs **1**–**5** and CCDC-182/213, CCDC-161428, CCDC-253084, CCDC-687762, the supplementary data of which can be obtained free of charge from The Cambridge Crystallographic Data Centre via www.ccdc.cam.ac.uk/data_request/cif).

(Figure 2a). To allow this H-bonding pattern to form, the isophthaloyl units of two adjacent molecules are stacked upon each other and the amide groups of **2** must be significantly tilted out of the overall macrocycle plane. The deviation from coplanarity of 44.4°[17] is unusually large for TLMs (Table 2). Quite interestingly, the same hydrogen-bonding motif has been observed recently for monolayers of **5** on Au(111) surfaces by ultrahigh-vacuum scanning tunneling microscopy (UHV-STM). The solid-state structure of **2** thus nicely supports the structural model that was based on the STM images and theoretical calculations of TLM trimers.[10] Variations of this pattern have been observed by STM: Two different types of domains have been observed in the monolayer of **5**, one in which infinite ladders of macrocycles cover the surface and one in which trimers of **5** exist with the same H-bonding pattern as that found in the crystal of **2**.[10]

In contrast to **2**, the 2-*in*-2-*out* conformation of **3** (**3B**) coexists in a 2:1 ratio with the corresponding all-*in* conformation (**3A**)[18] in the solid state. This results in a quite different hydrogen-bonding pattern: The two conformers are interconnected by intermolecular N–H···O=C bonds between all of the A_{out} protons of **3B** and all of the A_{in} oxygen atoms of **3A**. Thus, a hydrogen-bonded "copolymer" is formed, again as an infinite ladder (Figure 2b). Furthermore, the A_{in} protons of **3A** and **3B** interact with chloride anions.

In the X-ray crystal structure of $\mathbf{4}^+$, all of the solvent molecules and half of the counteranions cannot be fully resolved because they are disordered. The other half of the iodide anions can be located within the crystal lattice. Each of these iodide anions (I1 in Figure 1e) is connected to two TLMs through weak hydrogen bonds to their A_{in} protons (H4 in Figure 1e; Figure 3b). The intermolecular hydrogen-bonding pattern is quite unusual (Figure 3a and c), in that

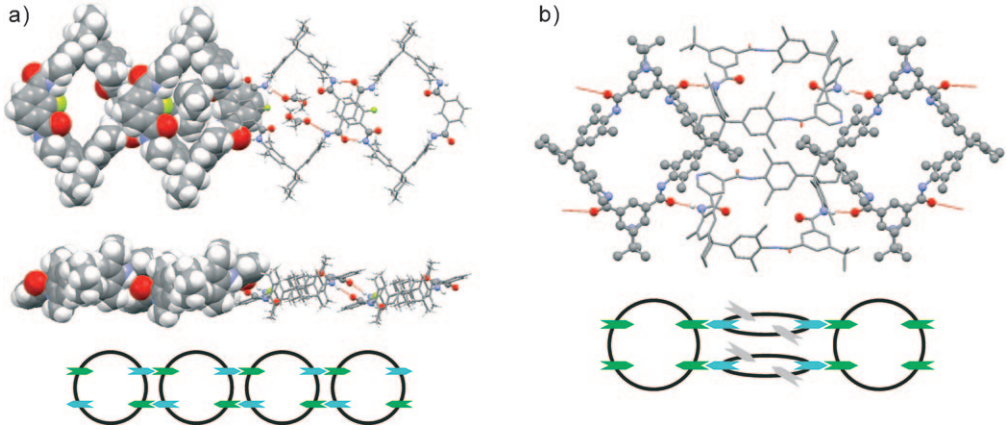

Figure 2. Hydrogen-bonding patterns of a) **2** and b) **3**, shown in a combination of stick, ball-and-stick, and space-filling representations (H atoms, except for the amide protons, are omitted for **3**). Hydrogen bonds appear as red, dotted lines. Color code: C gray, Cl green, F yellow, H white, I purple, N blue, O red. The cartoons illustrate the patterns in which amide groups are involved.

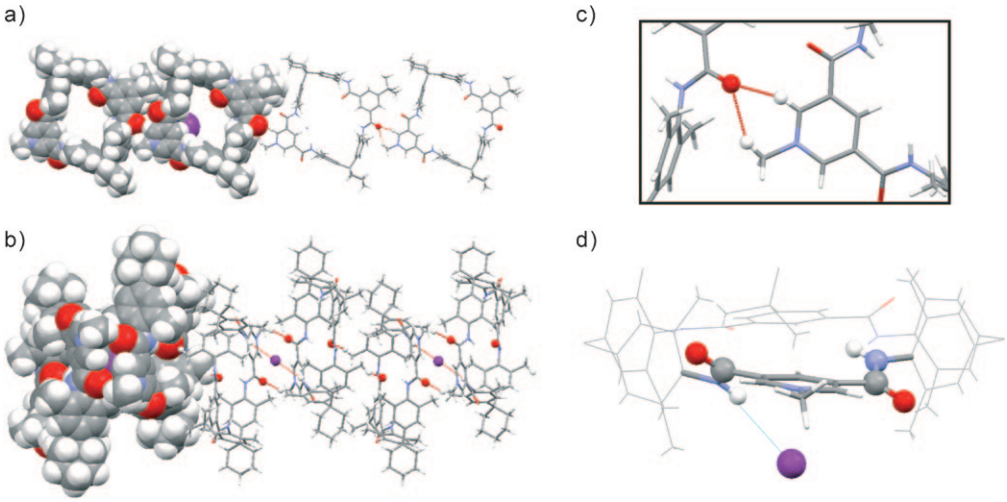

Figure 3. Hydrogen-bonding pattern of $\mathbf{4}^+$: a) View along crystallographic axis *c* and b) view along crystallographic axis *b*, shown in a combination of stick, ball-and-stick, and space-filling representations, with hydrogen bonds appearing as red, dotted lines. c) Enlarged view of the bifurcated C–H···O=C hydrogen bond of $\mathbf{4}^+$. d) View parallel to the macrocycle plane of $\mathbf{4}^+$, whch shows the two A_{in} groups pointing into different hemispheres that are separated by the macrocycle plane. Color code: C gray, Cl green, F yellow, H white, I purple, N blue, O red.

four C–H···O=C interactions are observed 1) between the A_{in} O1 oxygen atom and the pyridinium methyl H1 proton of the adjacent macrocycle, 2) between the A_{out} O3 oxygen atom and the *m*-xylyl methyl H3 proton, 3) between the A_{in} O2 oxygen atom and the pyridinium methyl H1 proton, and 4) between the A_{in} O2 oxygen atom and the pyridinium *ortho* H2 proton. Together with the N–H···I^- interactions, the first two hydrogen bonds build up an infinite zigzag stack of TLM $\mathbf{4}^+$ molecules (Figure 3b), whereas the last two interactions constitute a bifurcated hydrogen bond (Figure 3c) that leads to the assembly of an infinite chain within the crystal structure (Figure 3a). In addition, the fourth hydrogen bond is an exceptionally short C–H···O=C hydrogen bond (Table 1; d(H···O) = 2.16 Å, d(C–O) = 3.03 Å).[19] Together with the D–H···A angle of 151.8°, one can assume this bond to be relatively strong. N–H···O=C interactions are absent in the solid-state structure of $\mathbf{4}^+$. In particular, the seemingly predestined A_{out} H3 proton does not form any hydrogen bonds to adjacent TLMs, as it does in **2**, which thus indicates that the C–H···O=C bonds energetically compensate for the lack of N–H···O=C interactions.

A further remarkable finding in the X-ray crystal structure of $\mathbf{4}^+$ is the "divergence" of the two A_{in} groups bound to the pyridinium moiety. The proton of one A_{in} group points to the iodine atom on the lower side, while the proton of the other A_{in} group points to the upper side. Hence, they point into different hemispheres that are separated by the macrocycle plane (Figure 3d). This is unique because two A_{in} groups in the same isophthaloyl unit normally point into the same hemisphere, as observed in all other crystal structures of TLMs. The absence of rather strong H-acceptors (such as a carbonyl oxygen atom in ethyl acetate or a chloride anion) in the interior of the cavity could be a possible reason for this unusual conformational property of the amides.

In the crystal structure of **5**, the all-*in* conformation combined with the closed-doors conformation leads to a very interesting hydrogen-bonding motif: The H1 proton (Figure 1f) of the O1=C–N1H1 amide group forms an intermolecular hydrogen bond to the O1 oxygen atom, which is part of the same amide group, in the adjacent TLM (Figure 4a). The TLMs are arranged in a herringbone pattern with an angle of approximately 90° between them. In this manner, a quite remarkable catemer motif, [O=C–*N*–H···O=C–*N*–H···]$_\infty$, is obtained (Figure 4b and c).[20] The catemer motif is unprecedented in that the secondary amide group involved is an integral (and not peripheral) part of a macrocycle. This infinite chain of hydrogen bonds runs through the crystal along the "spine" of the herringbone motif, in marked contrast to the ladders observed for **2** and **3**, in which the hydrogen bonds are oriented more or less parallel with the ladder axis. Furthermore, this interaction is supported by a somewhat longer and therefore probably weaker N–H···O=C bond between the amide H2 proton and the same O1 oxygen atom. As a consequence of the hydrogen bonds, two of the four amide groups exhibit an unusually high deviation (50.3°) from coplanarity with the macrocycle plane, which

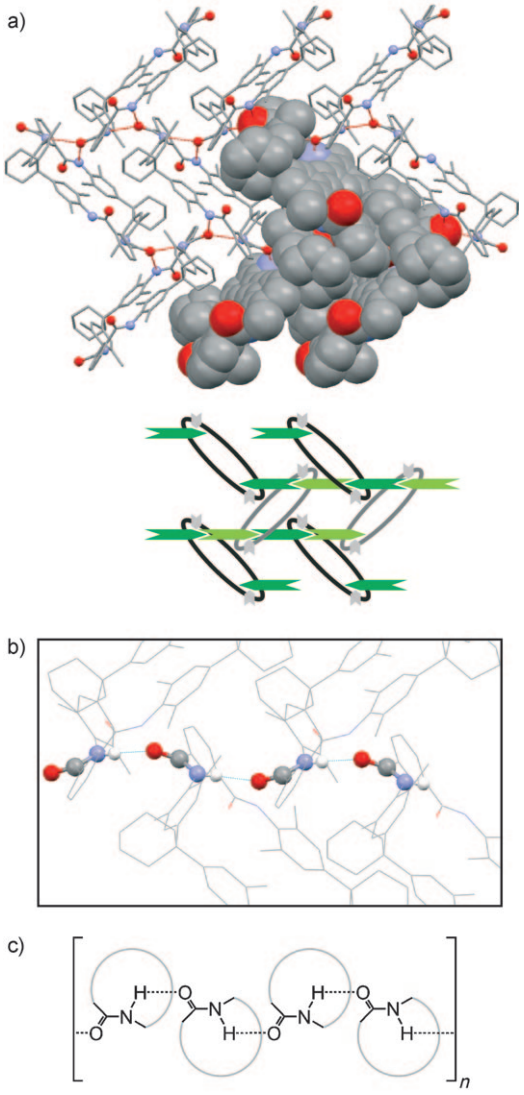

Figure 4. a) Hydrogen-bonding pattern of **5**, shown in a combination of stick, ball-and-stick, and space-filling representations (all H atoms omitted). A cartoon illustrates the patterns in which amide groups are involved. b) Enlarged view of the amide catemer motif in **5**. c) Schematic representation of this catemer motif. Color code: C gray, Cl green, F yellow, H white, I purple, N blue, O red.

is—to the best of our knowledge—the largest out-of-plane angle observed so far for TLMs in the solid state (Table 2).

The quite compact, intermolecular hydrogen-bonding patterns observed for **2** and **5** certainly depend on the conformational properties of the TLMs. Nevertheless, they are also determined by the substituents attached to the TLM periphery. For example, if R^1 (Scheme 1) in **2** were a *tert*-butyl group instead of a hydrogen atom, the overlapping pattern of the isophthaloyl units would probably be distorted and the structure observed for unsubstituted **2** might not form. The fact that a *tert*-butyl substituent disturbs such hydrogen-bonding patterns most likely contributes significantly to the much higher solubility of *tert*-butyl-substituted TLMs in unpolar solvents.

Conclusions

The detailed analysis of the solid-state structures of **1**–**5** uncovered several quite remarkable features of the TLMs under study. Although the overall macrocycle scaffold is quite rigid, it can easily adapt to the space requirements of guests inside the cavity because of the almost-free rotatability of the amide groups and the *m*-xylene rings. The TLM conformation changes significantly into the closed-doors structure when no guest is present. Together with the peripheral substituents, the conformational properties lead to a variety of interesting intermolecular hydrogen-bonding patterns. For instance, **5** reveals a notable catemer motif, whereas $\mathbf{4}^{+}$ exhibits several C−H···O=C interactions, including a remarkably short one. Our findings do not only provide support for previous theoretical predictions and STM experiments but will also be advantageous for crystal engineering. A more profound understanding of the rigidity/flexibility balance in TLMs will also help in the design of templated syntheses of supramolecular assemblies involving TLMs.

Experimental Section

General methods: Reagents were purchased from Sigma–Aldrich, Merck, or Fluka and used as received. Solvents such as dichloromethane and ethyl acetate were dried and distilled by the usual laboratory methods prior to use. Thin-layer chromatography (TLC) was carried out on TLC plates precoated with silica gel 60 F_{254} from Merck. Silica gel (0.04–0.063, 0.63–0.100 mm; Merck) was used for column chromatography. ^{1}H NMR and ^{13}C NMR spectra were recorded by using Bruker 250 and 500 MHz instruments. FAB-MS spectra were recorded by using a Concept 1H instrument from Kratos Analytical Ltd. with the matrix *m*-nitrobenzyl alcohol. ESI-MS spectra were recorded by using a Bruker APEX IV Fourier-transform ion-cyclotron-resonance (FT-ICR) mass spectrometer with an Apollo electrospray ion source equipped with an off-axis 70° spray needle. Melting points were determined with a Kofler Mikroskop-Heiztisch apparatus (Reichert). The following abbreviations are used: Ar: aryl; py: pyridyl; TLM: tetralactam macrocycle (with a generic structure as shown in Scheme 1). For the nomenclature of TLMs, see reference [21].

TLM 5: Compound **5** was synthesized according to the literature procedure.[1]

2-Fluoroisophthaloyl dichloride: This compound (used for the synthesis of compound **6**) was synthesized in three steps from 2,6-dimethylaniline. The aniline was first converted into 2-fluoro-*m*-xylene by a Schiemann reaction,[22] which was then oxidized with potassium permanganate to form 2-fluoroisophthalic acid.[23] In the last step, chlorination with sulfonyl chloride furnished 2-fluoroisophthaloyl dichloride.[24]

***N,N′*-Bis{4-[1-(4-amino-3,5-dimethylphenyl)cyclohexylidene]-2,6-dimethylphenyl}-2-fluoroisophthalamide (6)**: 1,1-Bis(4-amino-3,5-dimethylphenyl)cyclohexane (10 g, 31 mmol)[1,25] and triethylamine (1.4 mL) were dissolved in dry CH_2Cl_2 (50 mL). A solution of 2-fluoroisophthaloyl dichloride (1.08 g, 4.9 mmol) in dry CH_2Cl_2 (100 mL) was added dropwise over 4 h, while the system was kept under an argon atmosphere at room temperature. The mixture was left overnight with stirring. The solvents were then evaporated, and the product was isolated after column chromatography (silica gel, elution with $CHCl_3$/EtOAc (4:1)) as a colorless solid (2.7 g, 3.4 mmol, 69 %): R_f = 0.1 ($CHCl_3$/EtOAc (4:1)); m.p. 172–173 °C; ^{1}H NMR (250 MHz, $CDCl_3$): δ = 1.40–1.60 (br, 12H; CH_2), 2.10–2.30 (br, 8H; CH_2), 2.14 (s, 12H; ArCH_3), 2.25 (s, 12H; ArCH_3), 6.95 (s, 4H; Ar*H*), 7.02 (s, 4H; Ar*H*), 7.40 (t, ^{3}J(H,H) = 7.6 Hz, 1H; Ar*H*), 7.62 (s, 1H; N*H*), 7.67 (s, 1H; N*H*), 8.18 ppm (dd, ^{3}J(H,H) = 7.6 Hz, ^{4}J(H,F) = 7.6 Hz, 2H; Ar*H*); ^{13}C NMR (62.9 MHz, $CDCl_3$): δ = 18.1, 19.0, 23.0, 26.5, 37.2, 45.0, 121.5, 123.0, 123.2, 125.3, 127.0, 130.5, 134.7, 134.9, 137.6, 140.1, 149.0, 161.5 ppm; ^{19}F NMR (235 MHz, $CDCl_3$): δ = −117.15 ppm; FAB-MS: *m*/*z* (%): 792.4 (100) $[M+H]^{+}$.

TLM 2: A solution of isophthaloyl dichloride (264 mg, 1.3 mmol) in dry CH_2Cl_2 (250 mL) and a mixture of **6** (1031 mg, 1.3 mmol) and triethylamine (0.4 mL) in dry CH_2Cl_2 (250 mL) were simultaneously added dropwise to dry CH_2Cl_2 (1000 mL), while the system was kept under argon atmosphere. The addition was completed after 7 h, and the solution was left overnight with stirring. The solvents were evaporated, the residue was taken up in chloroform, and the solution was washed with water. The combined organic phases were dried over Na_2SO_4 and concentrated in vacuo. The residue was subjected to column chromatography (silica gel, elution with CH_2Cl_2/MeOH (25:1)), and 10^{2}-fluoro-7^{3},7^{5},13^{2},13^{6},20^{3},20^{5},26^{3},26^{5}-octamethyl-8,12,21,25-tetraaza-7,13,20,26-(1,4),10,23(1,3)-hexabenzenadispiro[5.7.5^{14}.7^{6}]hexacosaphane-9,11,22,24-tetrone (**2**) was obtained as a colorless solid (613 mg, 0.66 mmol, 51 %): R_f = 0.42 (CH_2Cl_2/MeOH (25:1)); m.p. >300 °C; ^{1}H NMR (250 MHz, $CDCl_3$/CD_3OD (5:1)): δ = 1.27 (br, 4H; CH_2), 1.36 (br, 8H; CH_2), 1.88 (s, 12H; ArCH_3), 1.90 (s, 12H; ArCH_3), 2.07 (br, 8H; CH_2), 6.68 (s, 4H; Ar*H*), 6.72 (s, 4H; Ar*H*), 7.14 (t, ^{3}J(H,H) = 7.8 Hz, 1H; Ar*H*), 7.37 (t, ^{3}J-(H,H) = 7.7 Hz, 1H; Ar*H*), 7.71 (dd, ^{3}J(H,H) = 7.2 Hz, ^{4}J(H,F) = 7.2 Hz, 2H; Ar*H*), 7.74 (dd, ^{3}J(H,H) = 7.7 Hz, ^{4}J(H,H) = 1.7 Hz, 2H; Ar*H*), 8.08 ppm (s, 1H; Ar*H*); ^{19}F NMR (235 MHz, $CDCl_3$/CD_3OD (5:1)): δ = −111.2 ppm; FAB-MS: *m*/*z* (%): 923.5 (100) $[M+H]^{+}$.

TLM $\mathbf{4}^{+}$: Methyl iodide (0.25 mL, 4 mmol) was added to a solution of TLM **3** (38.6 mg, 0.04 mmol)[13] in CH_3CN (2 mL) and $CHCl_3$ (0.5 mL). The mixture was left for 48 h with stirring. A yellowish precipitate was obtained, which was filtered and dried in vacuo to yield 23^{5}-*tert*-butyl-7^{3},7^{5},10^{5},13^{2},13^{6},20^{3},20^{5},26^{3},26^{5}-nonamethyl-8,12,21,25-tetraaza-10^{5}-azonia-7,13,20,26(1,4),10,23(1,3)-hexabenzenadispiro[5.7.5^{14}.7^{6}]hexacosaphane-9,11,22,24-tetrone iodide ($\mathbf{4}^{+}\mathrm{I}^{-}$) as a pale yellow solid (28.5 mg, 0.026 mmol, 65 %): M.p. >300 °C; ^{1}H NMR (500 MHz, [D_7]dimethylformamide ([D_7]DMF)): δ = 1.39 (s, 9H; C(CH_3)$_3$), 1.50 (br, 4H; CH_2), 1.62 (br, 8H; CH_2), 2.16 (s, 12H; ArCH_3), 2.21 (s, 12H; ArCH_3), 2.45–2.50 (br, 8H; CH_2), 4.81 (s, 3H; N^{+}CH_3), 7.22 (s, 4H; Ar*H*), 7.25 (s, 4H; Ar*H*), 8.18 (d, ^{4}J(H,H) = 1.5 Hz, 2H; Ar*H*), 8.74 (t, ^{4}J-(H,H) = 1.5 Hz, 1H; Ar*H*), 9.38 (br, 2H; N*H*), 9.70 (d, ^{4}J(H,H) = 1.2 Hz, 2H; Ar*H*(py)), 10.03 (br, 1H; Ar*H*(py)), 10.62 ppm (br, 2H; N*H*); ^{13}C NMR (125 MHz, [D_7]DMF): δ = 18.9, 19.1, 23.5, 26.8, 31.4, 32.4, 34.7, 45.5, 49.3, 119.3, 119.5, 126.3, 126.5, 128.5, 130.4, 132.6, 133.7, 134.1, 135.3, 135.5, 135.6, 144.0, 148.8, 153.0, 160.8, 165.7 ppm; FT-ICR-MS (ESI^{+}, from MeOH): *m*/*z* (%): 976.6 (100) $[M]^{+}$; HRMS (ESI^{+}): *m*/*z* calcd for $C_{64}H_{74}N_5O_4^{+}$: 976.5735 $[M]^{+}$; found: 976.5701.

X-ray crystallography: Single-crystal X-ray diffraction studies for TLMs $\mathbf{4}^{+}$ and **5** were carried out on a Nonius Kappa-CCD diffractometer at 100(2) K (**4**) and 123(2) K (**5**) with MoK_α radiation (λ = 0.71073 Å). Direct methods (SHELXS-97 software) were used for structure solution, and refinement was carried out by using the SHELXL-97 software (full-matrix least-squares on F^2). H atoms were localized by difference electron-density determination and refined by using a riding model (H(N) free) with the SHELX-97 software.[9]

X-ray crystallographic data for 1 (CCDC-Refcode: PIGDOY):[11] Colorless crystals; $C_{68}H_{80}N_4O_4{\cdot}3\,C_4H_8O_2{\cdot}2\,CH_2Cl_2$; M = 1451.5; crystal size 0.23 × 0.25 × 0.55 mm; triclinic; space group $P\bar{1}$ (no. 2); a = 11.616(4), b = 11.941(2), c = 15.920(3) Å; α = 71.95(2), β = 77.37(2), γ = 80.44(2)°; V = 2037.2(9) Å^3; Z = 1; ρ (calcd) = 1.183 mg m^{-3}; F(000) = 776; μ (Cu$_{K\alpha}$) = 1.77 mm^{-1}; T = 200(2) K; 6548 reflections measured ($2\theta_{max}$ = 120°); 6056 unique reflections (R_{int} = 0.117); 443 parameters; 409 restraint parameters; $R1$ ($I > 2\sigma(I)$) = 0.160; $wR2$ = 0.426 (all data). Due to the disordered solvent ($C_4H_8O_2$ and CH_2Cl_2) only the conformation, the nature of the inclusion, and the hydrogen-bond path between the host and the two included $C_4H_8O_2$ molecules could be determined.

X-ray crystallographic data for 2:[12] Colorless crystals, $C_{60}H_{63}FN_4O_4{\cdot}3\,C_4H_8O_2{\cdot}2\,CHCl_3$; M = 1426.19; crystal size 0.17 × 0.28 × 0.40 mm; triclinic; space group P-1 (no. 2); a = 11.325(1), b = 12.466(1), c = 13.983(1) Å; α = 85.06(1), β = 79.29(1), γ = 72.31(1)°; V = 1847.1(3) Å^3;

$Z=1$; ρ (calcd) $=1.282\ mg\,m^{-3}$; $F(000)=752$; μ (CuK_α) $=2.62\ mm^{-1}$; $T=293(2)$ K; 5781 reflections measured ($2\theta_{max}=120°$); 5487 unique reflections ($R_{int}=0.046$); 441 parameters, 111 restraint parameters; $R1$ ($I>2\sigma(I)$) $=0.123$; $wR2$ (all data) $=0.408$. TLM **2** crystallizes in a centrosymmetric space group with half a molecule in the asymmetric unit because the macrocycles are disordered in two directions. The fluorine substituent is, thus, randomly distributed over two inversion-related positions in the crystal.

X-ray crystallographic data for 4^+: Cuboid yellow crystals; $C_{64}H_{74}N_5O_4I_{0.5}$; $M=1040.73$; crystal size $0.12\times0.15\times0.19$ mm; monoclinic; space group $C12/c1$ (no. 15); $a=27{,}9903(5)$, $b=17.1774(3)$, $c=30.9747(6)$ Å; $\beta=107.148(1)°$; $V=14230.6(4)$ Å^3; $Z=8$; ρ (calcd) $=0.972\ mg\,m^{-3}$; $F(000)=4412$; μ (MoK_α) $=0.247\ mm^{-1}$; $T=100(2)$ K; 54127 reflections measured ($2\theta_{max}=55°$); 15809 unique reflections ($R_{int}=0.075$); 670 parameters; 0 restraint parameters; $R1$ ($I>2\sigma(I)$) $=0.0505$; $wR2$ (all data) $=0.1153$.

X-ray crystallographic data for 5: Colorless crystals; $C_{60}H_{64}N_4O_4$; $M=905.15$; crystal size $0.10\times0.20\times0.25$ mm; monoclinic; $P2_1/c$ (no. 14); $a=15.0288(2)$, $b=9.5142(1)$, $c=18.3963(2)$ Å; $\beta=108.246(1)°$; $V=2498.18(5)$ Å^3; $Z=2$; ρ (calcd) $=1.203\ mg\,m^{-3}$; $F(000)=968$; μ (MoK_α) $=0.075\ mm^{-1}$; $T=123(2)$ K; 35555 reflections measured ($2\theta_{max}=55°$); 5705 unique reflections ($R_{int}=0.048$); 317 parameters; 2 restraint parameters; $R1$ ($I>2\sigma(I)$) $=0.0383$; $wR2$ (all data) $=0.0975$.

CCDC-245578 (**2**), CCDC-687761 (**3**), CCDC-709648 (**4^+**), and CCDC-709644 (**5**) contain the supplementary crystallographic data for this paper. These data can be obtained free of charge from the Cambridge Crystallographic Data Centre via www.ccdc.cam.ac.uk/data_request/cif.

Acknowledgements

This research has been funded by the Deutsche Forschungsgemeinschaft (grant nos.: SFB 624 and SFB 765) and the Fonds der Chemischen Industrie (FCI). C.A.S. thanks the FCI for a Dozentenstipendium. S.S.Z. thanks the Studienstiftung des deutschen Volkes for a PhD scholarship.

[1] This type of macrocycle was first reported in: C. A. Hunter, *J. Chem. Soc. Chem. Commun.* **1991**, 749–751.
[2] F. Vögtle, S. Meier, R. Hoss, *Angew. Chem.* **1992**, *104*, 1628–1631; *Angew. Chem. Int. Ed. Engl.* **1992**, *31*, 1619–1622.
[3] Selected examples: a) S. Y. Chang, H. S. Kim, K. J. Chang, K. S. Jeong, *Org. Lett.* **2004**, *6*, 181–184; b) G. Kleefisch, C. Kreutz, J. Bargon, G. Silva, C. A. Schalley, *Sensors* **2004**, *4*, 136–146.
[4] Selected example: B. A. Blight, K. A. Van Noortwyk, J. A. Wisner, M. C. Jennings, *Angew. Chem.* **2005**, *117*, 1523–1528; *Angew. Chem. Int. Ed.* **2005**, *44*, 1499–1504.
[5] Selected examples: a) F. Vögtle, M. Händel, S. Meier, S. Ottens-Hildebrandt, F. Ott, T. Schmidt, *Liebigs Ann.* **1995**, 739–743; b) P. Linnartz, S. Bitter, C. A. Schalley, *Eur. J. Org. Chem.* **2003**, 4819–4829; c) P. Ghosh, G. Federwisch, M. Kogej, C. A. Schalley, D. Haase, W. Saak, A. Lützen, R. M. Gschwind, *Org. Biomol. Chem.* **2005**, *3*, 2691–2700; d) B. A. Blight, X. Wei, J. A. Wisner, M. C. Jennings, *Inorg. Chem.* **2007**, *46*, 8445–8447.
[6] Selected examples: a) C. A. Hunter, *J. Am. Chem. Soc.* **1992**, *114*, 5303–5311; b) Q. Y. Li, E. Vogel, A. H. Parham, M. Nieger, M. Bolte, R. Frohlich, P. Saarenketo, K. Rissanen, F. Vögtle, *Eur. J. Org. Chem.* **2001**, 4041–4049; c) X. Y. Li, J. Illigen, M. Nieger, S. Michel, C. A. Schalley, *Chem. Eur. J.* **2003**, *9*, 1332–1347.
[7] a) W. Reckien, S. Peyerimhoff, *J. Phys. Chem. A* **2003**, *107*, 9634–9640; b) C. A. Schalley, W. Reckien, S. Peyerimhoff, B. Baytekin, F. Vögtle, *Chem. Eur. J.* **2004**, *10*, 4777–4789.
[8] If the macrocycle is divided into two halves by a plane bisecting the two isophthalamides, we can distinguish one 2-*in*-2-*out* conformation, in which the A_{out} groups lie in the same half, from another 2-*in*-2-*out* conformation, in which the A_{out} groups lie in different halves. The latter is observed in the crystal structures.
[9] G. M. Sheldrick, *Acta Crystallogr. Sect. A* **2008**, *64*, 112–122.
[10] I. Kossev, W. Reckien, B. Kirchner, T. Felder, M. Nieger, C. A. Schalley, F. Vögtle, M. Sokolowski, *Adv. Funct. Mater.* **2007**, *17*, 513–519.
[11] C. Fischer, M. Nieger, O. Mogck, V. Böhmer, R. Ungaro, F. Vögtle, *Eur. J. Org. Chem.* **1998**, 155–161.
[12] M. Nieger, T. Schmidt, F. Vögtle, private communication, **2004**, CCDC-245578 (CCDC-Refcode: YAFDOZ). TLM **2** was crystallized by slow evaporation of the solvents $CHCl_3$/EtOAc.
[13] B. Baytekin, S. S. Zhu, B. Brusilowskij, J. Illigen, J. Ranta, J. Huuskonen, K. Rissanen, L. Kaufmann, C. A. Schalley, *Chem. Eur. J.* **2008**, *14*, 10012–10028.
[14] a) P. Ghosh, G. Federwisch, M. Kogej, C. A. Schalley, D. Haase, W. Saak, A. Lützen, R. M. Gschwind, *Org. Biomol. Chem.* **2005**, *3*, 2691–2700; b) B. A. Blight, J. A. Wisner, M. C. Jennings, *Chem. Commun.* **2006**, 4593–4595.
[15] H. Adams, F. J. Carver, C. A. Hunter, *J. Chem. Soc. Chem. Commun.* **1995**, 809–810.
[16] The macrocycle plane is defined by the least-squares fit plane through the two quaternary cyclohexane carbon atoms and the four amide α-carbon atoms.
[17] 44.4° is the angle between the plane of the A_{out} groups (formed by the four atoms H13, N13, C14, and O14) and the macrocycle plane of **2**. With regard to all of the crystal structures of TLMs, this is the largest angle between the plane of an A_{out} amide group and the macrocycle plane.
[18] Compound **3** crystallizes in a centrosymmetric space group, and in the crystal structure, the all-*in* conformer **3A** is disordered in terms of the position of the pyridine group and the *tert*-butylbenzene group.
[19] To the best of our knowledge, no other example for a similarly short aryl-C–H···O=C–NH hydrogen bond is known. A comparably short hydrogen bond with a carboxylate oxygen atom as the acceptor has been reported in: A. Abu-Rayyana, Q. Abu-Salem, N. Kuhn, C. Maichle-Mossmer, E. Mallah, M. Steimann, *Z. Naturforsch. B* **2008**, *63*, 1015–1019. Calculations on comparable hydrogen bonds with methyl C–H groups as the donors have been reported in: C. E. Cannizzaro, K. N. Houk, *J. Am. Chem. Soc.* **2002**, *124*, 7163–7169.
[20] For related amide catemers, see: S. S. Kuduva, D. Bläser, R. Boese, G. R. Desiraju, *J. Org. Chem.* **2001**, *66*, 1621–1626.
[21] H. A. Favre, D. Hellwinkel, W. H. Powell, H. A. Smith, S. S. C. Tsay, *Pure Appl. Chem.* **2002**, *74*, 809–834.
[22] M. S. Nasir, B. I. Cohen, K. D. Karlin, *J. Am. Chem. Soc.* **1992**, *114*, 2482–2494.
[23] J. W. Ladbury, C. F. Cullis, *Chem. Rev.* **1958**, *58*, 403–438, and references therein.
[24] K. M. Doxsee, M. Feigel, K. D. Stewart, J. W. Canary, C. B. Knobler, D. J. Cram, *J. Am. Chem. Soc.* **1987**, *109*, 3098–3107.
[25] C. A. Hunter, *J. Am. Chem. Soc.* **1992**, *114*, 5303–5311.

Received: February 6, 2009
Published online: April 16, 2009

